Supplementary Information For:

Electron-nuclear decoupling at a spin clock transition

Krishnendu Kundu,[1] Jia Chen,[2,3,4] Silas Hoffman,[2,3,4,*] Jonathan Marbey,[1,4,5] Dorsa Komijani,[1,5] Yan Duan,[6] Alejandro Gaita-Ariño,[6] John Stanton,[3,4,7] Xiaoguang Zhang,[2,3,4] Hai-Ping Cheng,[2,3,4,*] Stephen Hill[1,4,5,*]

[1]*National High Magnetic Field Laboratory, Florida State University, Tallahassee, FL 32310, USA*

[2]*Department of Physics, University of Florida, Gainesville, FL 32611, USA*

[3]*Quantum Theory Project, University of Florida, Gainesville, FL 32611, USA*

[4]*Center for Molecular Magnetic Quantum Materials, University of Florida, Gainesville, FL 32611, USA*

[5]*Department of Physics, Florida State University, Tallahassee, FL 32306, USA*

[6]*Instituto de Ciencia Molecular (ICMol), Universidad de Valencia, Paterna, Spain*

[7]*Department of Chemistry, University of Florida, Gainesville, FL 32611, USA*

[*]**Email:** silas.hoffman@ufl.edu, hping@ufl.edu, shill@magnet.fsu.edu

Contents

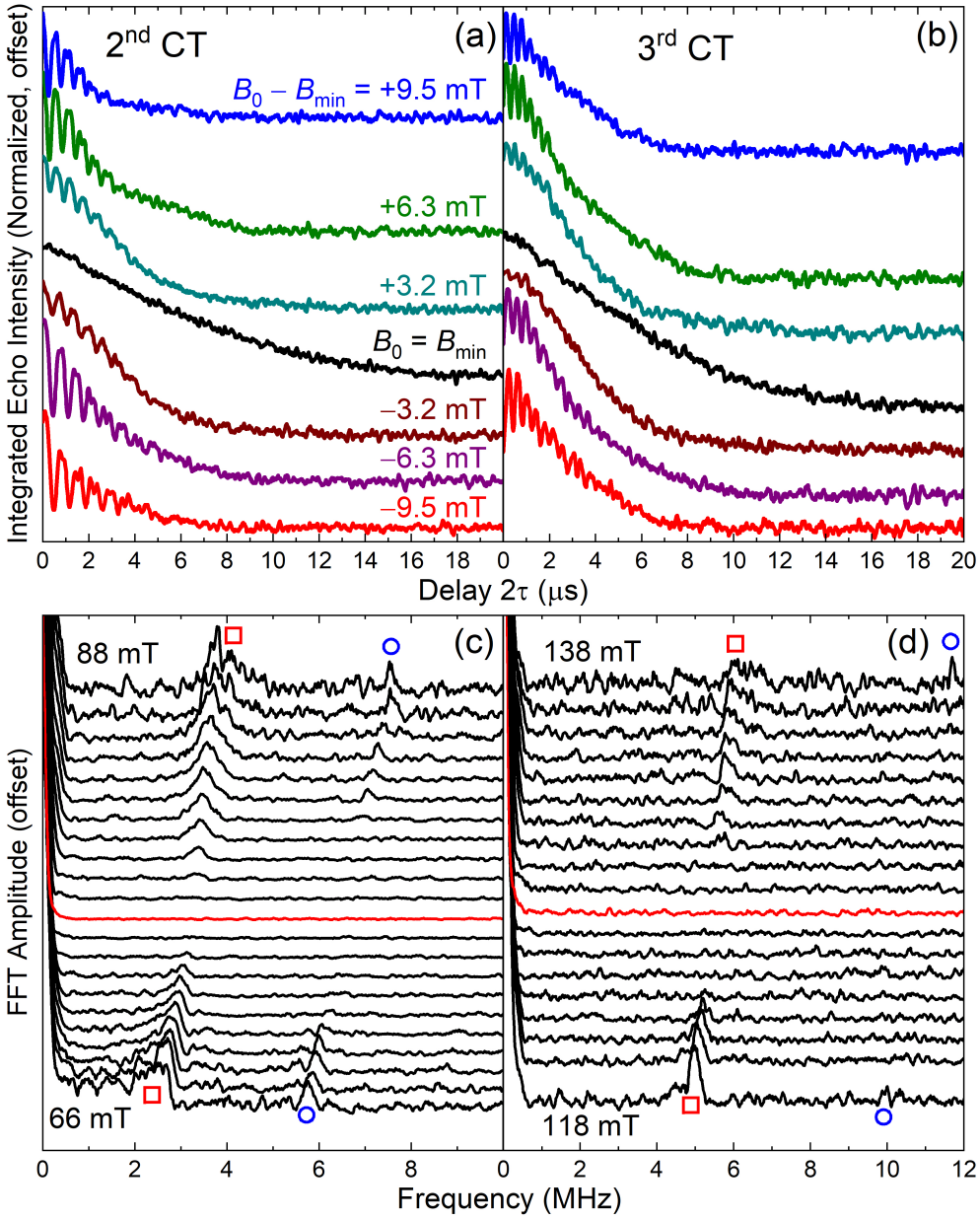

Figure S1. Electron spin-echo decay curves recorded for HoW_{10} at 9.18 GHz and 5 K as a function of detuning, $B_0 - B_{\min}$ (see labeling), in the vicinity of the 2^{nd} (a) and 3^{rd} (b) clock transitions (CTs) at $B_{\min} = 76.6$ mT and 127.6 mT, respectively. Corresponding Fast Fourier Transforms (FFTs) of the echo decay curves at the 2^{nd} (c) and 3^{rd} (d) CTs, recorded in 1.05 mT steps from 66 to 88 mT and 118 to 138 mT, respectively; not all of the echo decay curves are displayed in (a) and (b). The red squares and blue circles denote ESEEM peaks at the 1^{st} and 2^{nd} harmonics of the proton Larmor frequency, ν_{H}, and the red curves correspond exactly to the CTs.

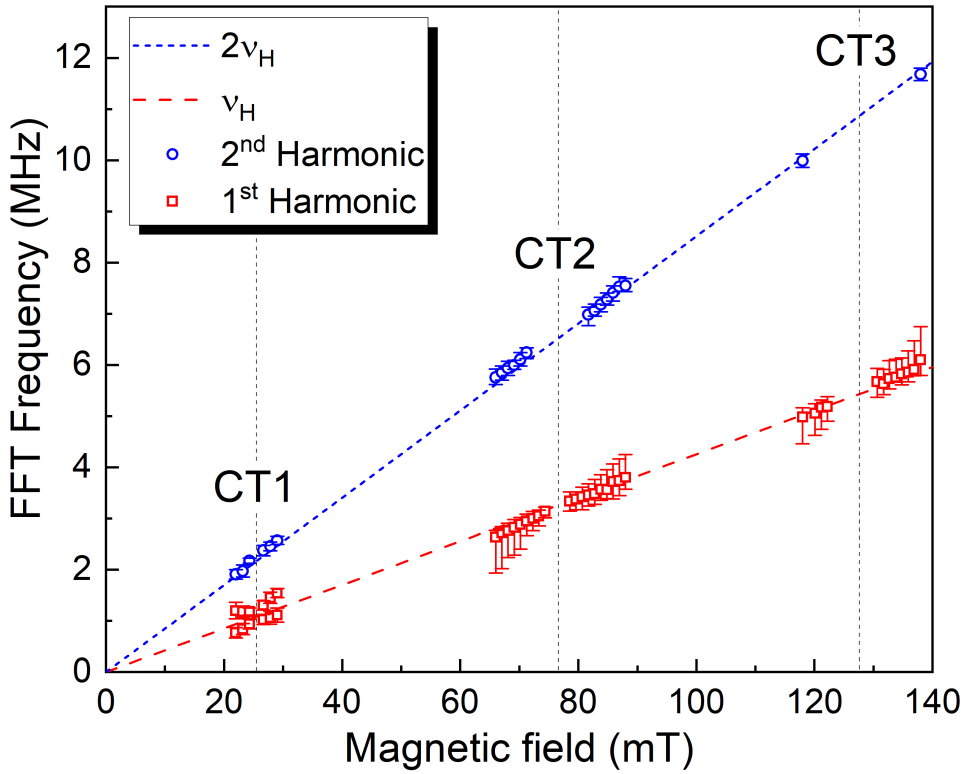

Figure S2. Plot of ESEEM frequencies versus B_0 at the 1^{st} (CT1), 2^{nd} (CT2) and 3^{rd} (CT3) clock transitions, determined from the FFT spectra in Figure 2(b) (main article) and Figure S1 (c,d). The error bars at CT1 denote $\pm$s.d. (approximating each peak as a Gaussian), while those at CT2 and CT3 denote the half widths at half the maximum amplitude. In all cases, the data points represent the frequency at which the maximum FFT amplitude is observed. The colored dashed lines and the colors/shapes of the data points distinguish the 1^{st} and 2^{nd} harmonics of the proton Larmor frequency, ν_H (see legend), while the vertical dashed lines indicate the exact locations of the three clock transitions.

Supplementary Discussion

The ESEEM data recorded at the 2^{nd} and 3^{rd} clock transitions (Figures S1 and S2) display near identical trends to those observed at the 1^{st} (see Figure 2, main article). The main differences are

the increases in the frequencies of the harmonic content at successive clock transitions, along with diminishing amplitudes relative to the overall echo intensity. The former is seen even via simple visual inspection of the echo decay curves. However, the trend is most clearly observed in Figure S2, where the harmonic content of the FFT frequencies lie on the straight lines corresponding to the 1^{st} and 2^{nd} harmonics of the proton Larmor frequency, ν_{H}, which obviously scale linearly with B_0. The diminishing amplitudes are also easily understood on the basis of the discussion given in the main article. First and foremost, the ESEEM is only observed clearly in proximity to the clock transitions because of the enhanced phase memory times in these field regions. Second, the effective electron gyromagnetic ratio, $\gamma_{\mathrm{e}}^{\mathrm{eff}}$, is less than 0.5 MHz in the regions close to each CT. It is this interaction scale that controls the ESEEM modulation depth: strong modulations are observed when $\gamma_{\mathrm{e}}^{\mathrm{eff}} \approx \nu_{\mathrm{H}}$; meanwhile, the modulation depth decreases as ν_{H} increases relative to $\gamma_{\mathrm{e}}^{\mathrm{eff}}$. Thus, it is easily seen from Figure S2 that the ESEEM will be strongest at CT1, where $\nu_{\mathrm{H}} \approx 1$ MHz, and weakest at CT3, where $\nu_{\mathrm{H}} \approx 5$ MHz. Indeed, no ESEEM was discernible at the 4^{th} clock transition in these investigations, presumably because ν_{H} is too large relative to $\gamma_{\mathrm{e}}^{\mathrm{eff}}$.

The other main difference between the data in Figures S1 and S2 relative to those in the main article is that a clear peak splitting is not observed in the 1^{st} harmonic at CT2 and CT3. The reason for this has been discussed in Ref. [1]. Orientational disorder in the crystals leads to a distribution in clock transition fields, B_{min}, with the effect being more pronounced with increasing applied field, B_0. This is seen most clearly in the divergence of T_{m} in Figure 3 of Ref. [1], which is very sharp at CT1 and becomes broader at successive clock transitions. This broadening mechanism also leads to increased smearing of the ESEEM frequencies at successive clock transitions, which

has two effects: firstly, it will prevent resolution of the 1^{st} harmonic peak splitting; second, it represents a second factor leading to a diminishing of the ESEEM modulation depth at successive clock transitions. However, it is clear that the 1^{st} harmonic FFT peaks broaden upon moving away from CT2 and CT3, as best illustrated by the error bars in Figure S2. This suggests that there is an unresolved peak splitting that increases as A^{eff} increases upon moving away from each clock transition. Finally, the main observation of this study, namely the vanishing of electron-nuclear coupling, is clearly borne out at CT1, CT2 and CT3 for HoW_{10}.

Supplementary References

1. Shiddiq, M. *et al.* Enhancing coherence in molecular spin qubits via atomic clock transitions. *Nature* **531**, 348–351 (2016). URL `https://doi.org/10.1038/nature16984`.